Journal of Hydrology 365 (2009) 95–104

Contents lists available at ScienceDirect

Journal of Hydrology

journal homepage: www.elsevier.com/locate/jhydrol

Optimized groundwater drawdown in a subsiding urban mining area

Peter Bayer [a,*], Emre Duran [b], Rainer Baumann [c], Michael Finkel [b]

[a] *Institute of Environmental Engineering, Ecological Systems Design, ETH Zurich, HIF C 43, Schafmattstrasse 6, CH-8093 Zurich, Switzerland*
[b] *Center for Applied Geosciences, University of Tübingen, Sigwartstrasse 10, D-72076 Tübingen, Germany*
[c] *Emschergenossenschaft, Kronprinzenstrasse 24, D-45128 Essen, Germany*

ARTICLE INFO

Article history:
Received 16 April 2008
Received in revised form 8 September 2008
Accepted 19 November 2008

Keywords:
Groundwater
Mining
Optimization
Evolutionary algorithms
CMA-ES

SUMMARY

This study establishes the first real-world application of evolution strategies for solving a groundwater management problem. In an urban coal mining area in the Emscher and Rhine Basin of Northwestern Germany the groundwater table rises relative to subsiding ground and threatens local infrastructure and basements of buildings. The active extraction system, which consists of one highly productive horizontal and twelve vertical wells that pump more than 500 m^3/h, is revised by combining groundwater model and algorithmic optimization procedure. By capitalizing on the robustness and self-adaptivity of evolution strategies, both fixed and moving well formulations are solved. It is shown that well layout can be improved by automatic optimization even though it has been previously soundly configured by experts. The total pumping effort can be noticeably reduced while complying with the drawdown targets given at 24 different locations in the study area. Savings increase if new well positions are considered. For example, one additional well yields a 9% reduction of the total extraction rate. We also investigate the relevance of the spatially variable drawdown targets and demonstrate how those targets that mainly control the optimized well layouts can be identified by varying the penalty function. It is revealed that there is huge potential for additionally reducing the extraction rate if one or more of these individual targets could be resigned, for example as a result of technical construction or land use changes. A reduction of more than 25% has been estimated for giving up the most notable constraining target. This way, by testing the significance of given constraints, algorithmic optimization may guide the re-formulation of the original optimization problem in order to conceive new groundwater management scenarios that ultimately lead to an increased efficiency of the well field. This procedure is similar to a chance-constraint approach, efficient with CMA-ES, but can be adopted in any other combined hydrological simulation–optimization problem.

Introduction

As a consequence of centuries of impacting on natural aquifers and exploitation of the reserves of the subsurface, and under current climate changes, numerous urban areas now suffer severe and irreversible remote damage. The withdrawal of groundwater through well pumping has led to subsidence in such cities as Mexico City, Bangkok and Venice (Morton, 2003; Carbognin et al., 2004; Phien-wej et al., 2006). Another issue is the compaction or collapse of former salt and coal mines, as has been observed in the mining areas of central Europe (Roosmann et al., 2003; Baumgart et al., 2003). Even though years have passed since mining activities ceased, subsidence is still slowly continuing in some regions. Lowered ground surfaces induce a relative rise of the groundwater table, which represents a risk for buildings and urban infrastructure.

Due to the lack or infeasibility of more sustainable technical solutions (e.g., Marino and Abdel-Maksoud, 2006), drainage or continuous pumping systems that artificially keep the water table low are commonly employed. Applying and maintaining these technologies is an enormous endeavor, with a huge amount of effort and expense involved. This, in turn, means that even small improvements made by fine-tuning existing technological arrangements can yield substantial cost savings. The presented study deals with model-based optimization of an existing well field in the former mining area at the Ruhr Basin in Germany. We demonstrate how combined simulation–optimization can be utilized to revise the currently active well scheme so that the required permanent groundwater extraction rate can be effectively minimized.

Combined simulation–optimization has been applied to a variety of hydrogeological control problems and has proven to be particularly beneficial for demanding, complex problems that can hardly be solved by trial-and-error methods or manual tuning

* Corresponding author. Tel.: +41 44 6337639; fax: +41 44 6331061.
E-mail addresses: bayer@ifu.baug.ethz.ch (P. Bayer), emred81@yahoo.com (E. Duran), baumann.rainer@eglv.de (R. Baumann), michael.finkel@uni-tuebingen.de (M. Finkel).

0022-1694/$ - see front matter © 2008 Elsevier B.V. All rights reserved.
doi:10.1016/j.jhydrol.2008.11.028

alone (e.g., Freeze and Gorelick, 1999; Zheng and Wang, 2002; Park and Aral, 2004; Chu et al., 2005; Katsifarakis and Petala, 2006; Mantoglou and Kourakos, 2007; Papadopoulou et al., 2007; Bürger et al., 2007; Bayer et al., 2008). Such problems include the simultaneous adaptation of positions and discharge rates of multiple wells in heterogeneous aquifers (e.g., Guan and Aral, 1999; Bayer and Finkel, 2004), an issue which is also addressed in the presented study. Combined simulation–optimization typically involves solving an objective function by utilizing the output of a numerical model. The model is applied to test the performance of a selected well layout. The objective function is solved by an external solver, an evolutionary algorithm, for instance. Such a heuristic solver is particularly suitable when objective functions are expected to have several local optima. The evolutionary algorithm selected here, the so-called evolution strategy, has been shown to exhibit substantial global search capacities to cope with potential non-convexities of objective functions (Bayer and Finkel, 2004, 2007; Bürger et al., 2007). However, no real case application is currently available. This is subject of this study. Theoretical findings about the applicability of evolution strategies are transferred into practice by optimizing a large-scale well field. Special attention is drawn to the formulation of constraints and their effect on the optimized well layout. This is an uncommon approach, since it means utilizing variations of the problem formulation in order to inspect the sensitivity of the optimized solution. Hence, the combined simulation-optimized concept is not only used for identifying one optimal solution but for comparing conditioned alternatives. Contrasting solution alternatives can substantially improve complex system understanding and will ultimately ease transfer into practice. However, such a procedure requires also a robust and unspecific, ideally adaptive solver. In principle, an evolution strategy such as the CMA-ES should be an ideal candidate.

In the subsequent chapter, the study site and the groundwater model set up are presented. The layout of the existing well field is referred to as "reference case". In order to analyze the possibilities of revising the reference case, we then introduce three different optimization problems that are separately examined. The individual problems differ with respect to acceptable well positions to fulfill predefined minimum drawdown constraints. Of particular importance is the total extraction rate that represents the main economic determinant. Varying the degree of freedom for both well positions and drawdown constraints is shown to influence the optimized layouts. Based on this variation procedure, sensitive elements of the optimization problem (wells, constraints) can be identified, enabling us to settle on those modifications that exhibit highest potential for further developing the extraction system. Further, it is shown how examination of the significance of given drawdown targets, which constrain the optimization problem, may offer new alternatives for improving the existing groundwater management.

Study area and groundwater model

The study area, Aldenrade-Walsum (Fig. 1) in the city of Duisburg, is a subsidence area of one of the last active stone coal mines in the Emscher catchment area of Germany. Large-scale underground mining began after finishing the first shaft sinking operation in 1930, and a second shaft was finished around 1937. The annual coal production from Walsum mine reached 1.5 million tons by the end of 1943. During the Second World War, mining was disturbed and part of the mine was destroyed. Following reconstruction, the second shaft sinking operation was completed (1954–1955). After 1968, mechanization and rationalization of mining created a yield of 3 million tons of coal per year. The mine reached its largest capacity in 1993. In this year, final closure plans were discussed for the first time. Several old shafts were closed down in the following years, and the complete closure of Walsum mine was planned for June 2008. Currently, the mine delivers 2.5 million tons of coal per year, with approximately 3000 workers (DSK, 2002).

The sequence of the strata in the study area is as follows (Fig. 2): carbon rocks are found 100–130 m below the surface and are formed by clay-and-silt rocks and sandstones that host the coal seam. The overlying layers are upper Cretaceous at depths between 90 and 115 m. These are overlaid by the tertiary formations, the younger rocks of which are partially eroded. The young tertiary Hamborn layer is composed of plastic clays, silts, and light fine sand. The clays and the silts act as an aquitard at the base of the upper quaternary aquifer. The quaternary formations represent

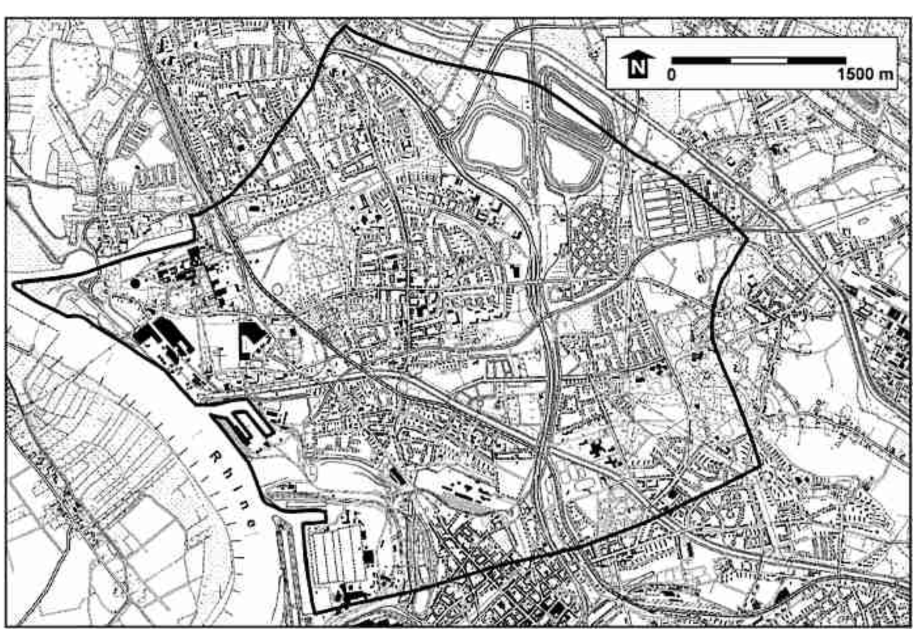

Figure 1. Map of the Walsum site of Aldenrade/Duisburg (Germany) and the boundaries of the numerical model demarcated as bold line.

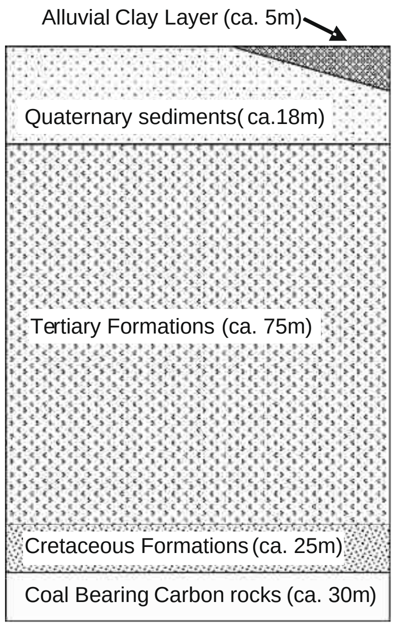

Figure 2. Scheme of stratigraphical cross-section of study area.

heterogeneous, highly permeable sandy sediments from the terrace of the Rhine River.

As is common for many former underground mining regions, the main problem affecting the Walsum mine area is the ground subsidence as a consequence of the mining operations. The subsidence is mainly caused by sinking of the quaternary sediments overlying the mined out zone. Major problems resulting from subsidence in this high-density area are the amplified danger of floods from the adjacent Rhine River as well as the increasing risk of wetting or flooding of the basements of buildings due to the relative rise of the groundwater table. To remedy the situation, the first permanent groundwater drainage and extraction system was put into operation in 1975. This first system was subsequently expanded to its present size. The current system consists of 13 wells, 12 vertical and 1 horizontal, sited in the upper quaternary aquifer. The drawdown is focused on the area of highest subsidence (see "area of interest" as delineated in Fig. 3).

In order to simulate the hydrogeological conditions in the quaternary aquifer, a two-dimensional groundwater flow model of the main aquifer has been set up. The model is implemented in the finite-element-based modeling software SPRING (SPRING, 2004). The model is calibrated for steady state as well as for transient conditions (Emschergenossenschaft, 2004). For the transient calibration, a long term pumping test over a period of one month was realized (DMT, 2005). The model area extends from the river Emscher in the north along the harbor Walsum und the river Rhine up to Duisburg-Aldenrade/-Fahrn in the south. The eastern boundary is defined as the lower terrace of the river Rhine (Fig. 1). The complete model area includes around 17 km^2. With this model layout there is no influence on the modeling results leading back to the model boundaries. The finite-element grid is shown in Fig. 3. All lateral boundaries of the model domain are expressed as constant heads. The hydraulic conductivities (K) in the model characterize those of the quaternary deposits which range from 9×10^{-3} m/s to 2×10^{-6} m/s with the spatial distribution of $\log(K)$ depicted in Fig. 4.

The twelve vertical wells are numbered by nodes W1–12, whereas the horizontal well, W13, is represented by 11 neighboring nodes. The total extraction rate $Q_{tot,ref}$ is currently 543 m^3/h, which is used as a reference value for all other cases considered in this study. As illustrated in Fig. 5, we can distinguish three major well groups: Wells W1–6 in the northwestern part contribute 36%

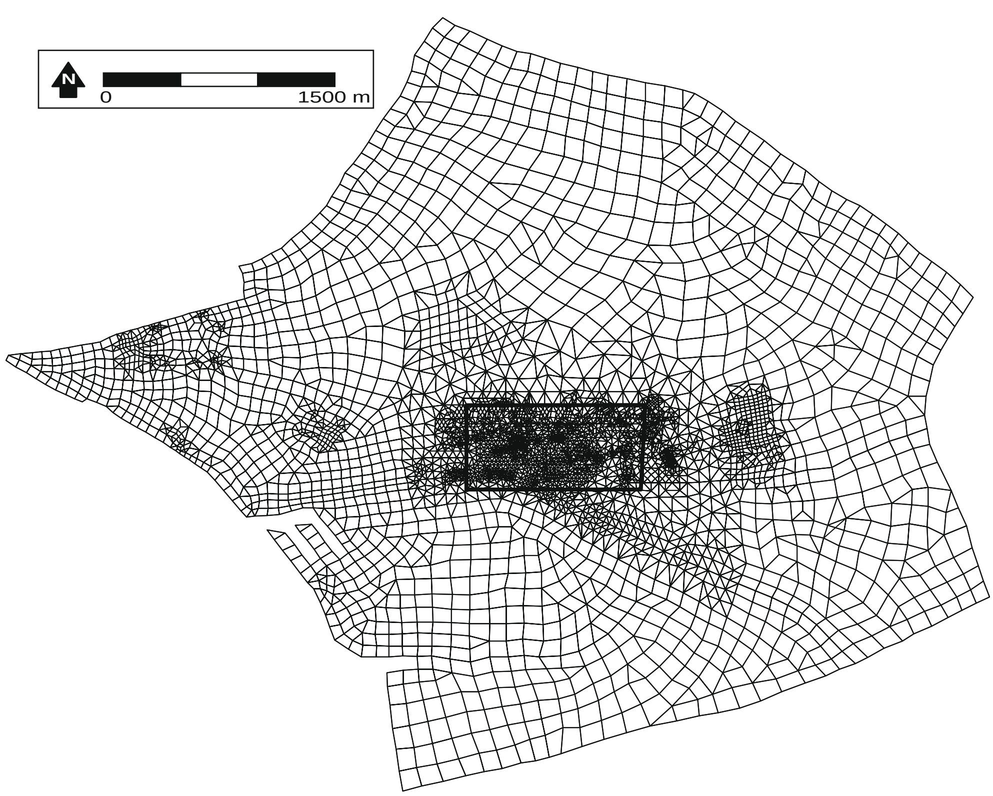

Figure 3. Finite-element grid of SPRING model for Walsum site; bold rectangular area in the center delineates the "area of interest".

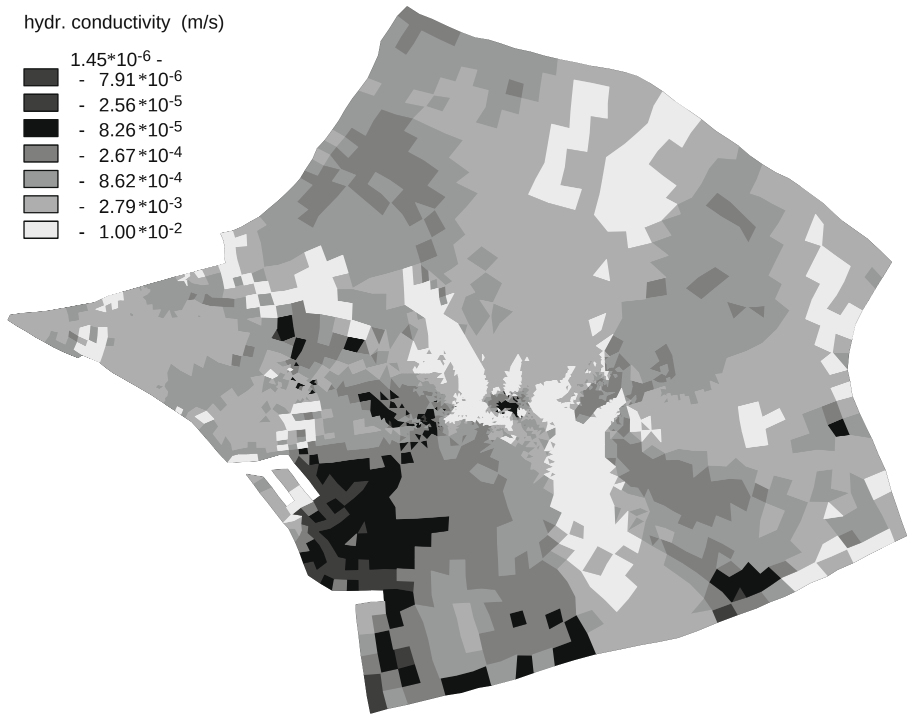

Figure 4. Spatial hydraulic conductivity distribution of two-dimensional Walsum model.

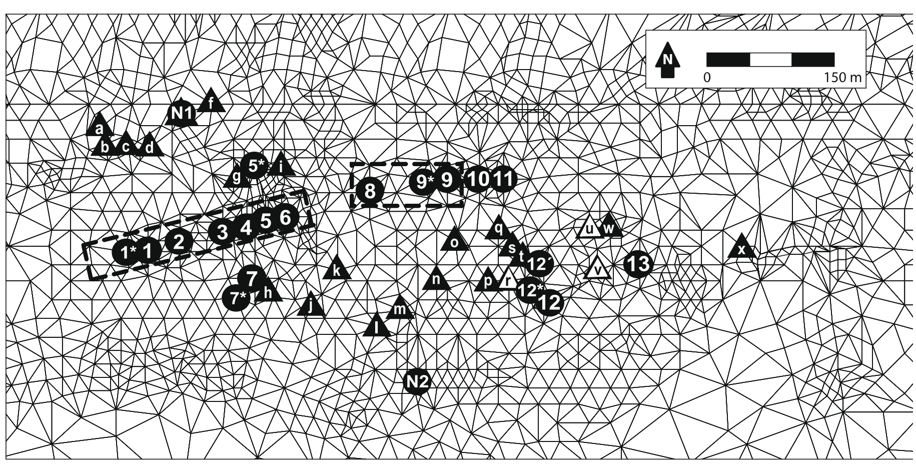

Figure 5. Zoomed central section of model (see Fig. 2) representing the area of interest with model grid, (numeric) well locations and (alphabetic) constraint positions. Existing wells are named W1–13, and potential new well positions are named N1, N2 and W1*, W5*, W7*, W12*, and W12'. Dashed lines delineate well placement areas of fixed and moving well case MW_{small}.

to Q_{tot}, wells W8–11 in the central northern area contribute 16% and the eastern horizontal well W13, 43%. Further insulated wells, W7 and W12 in the south, are of minor relevance for Q_{tot} of the existing system. Fig. 6 depicts the head contours in the area of interest with the most pronounced local drawdown around the northwest well gallery and W7, as well as at W13 in the east. In this figure, those nodes are highlighted where predefined maximum groundwater levels have to be achieved. The groundwater table is lowered by up to more than 2 m to comply with the drawdown targets, which are predefined at 24 locations (see alphabetically labeled nodes in Figs. 5 and 6).

Problem formulation and solution

The main goal of this study is to combine and optimize the drawdown targets at minimum total pumping rate Q_{tot}, which is the sum of the individual pumping rates of the existing wells at fixed positions and of possible new wells that may be envisioned in addition to the existing ones. The objective function to be solved is stated as

$$F(Q,x,y) = \left[\sum_{i=1}^{13} Q_i^{old} + \sum_{j=1}^{J} Q_j^{new}(x_j,y_j)\right]\cdot P \tag{1}$$

$$Q_{i,low}^{old} \leqslant Q_i^{old} \leqslant Q_{i,up}^{old} \tag{2}$$

$$Q_{j,low}^{new} \leqslant Q_j^{new} \leqslant Q_{j,up}^{new} \tag{3}$$

$$x_{j,low} \leqslant x_j \leqslant x_{j,up} \tag{4}$$

$$y_{j,low} \leqslant y_j \leqslant y_{j,up} \tag{5}$$

where Q denotes the pumping rates with indices i for existing ($Q^{old}, W1,\ldots,W13$) and j for new wells (Q^{new}). Parameter P represents the penalty term that will explicitly be defined below. The

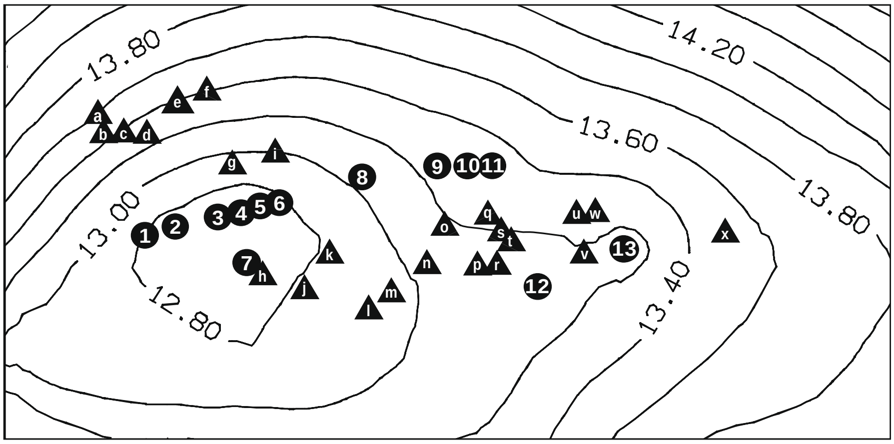

Figure 6. Head contours within "area of interest" for reference case; the wells W1–13 are depicted as circles, 'a–x' in triangles denotes the constraint location where water table maxima are set.

objective function F (Eq. (1)) has to be adjusted according to the nature of new wells (if required). In the following, we distinguish between the existing situation (serving as reference case) and three further optimization cases with individually adjusted objective function formulations. For the "*fixed wells*" case, (subsequently denoted as FW), no further wells are considered ($J = 0$) and only the pumping rates Q_i^{old} of the existing wells are adapted. The lower limit, $Q_{i,low}^{old}$, is set at 5% of the well-specific extraction rate in the reference case and the upper limit is set at 110% (Eq. (2)). The latter reflects that all existing wells are already operating close to the maximum capacity.

Two further optimization cases consider the installation of one or more additional wells ("*fixed and moving well*" cases, MW_{big} and MW_{small}). For these, $J \geqslant 1$ in objective function F as given by Eq. (1). The limits for Q_i^{old} are the same as for the case "*fixed wells*". The case MW_{small} takes into account the specific conditions within the area of interest with respect to existing buildings and local connections to channels, which direct the extracted water to the Rhine River. Well placement areas are limited to relatively small areas and locations that are particularly favorable for installing new wells. As shown in Fig. 5, two of these placement areas are located along the existing north-eastern well gallery and around wells W8 and W9. The well position in the first area is expressed by assuming only one decision variable, x_j, denotes the position along the line depicted in Fig. 5. The small rectangular northern well placement area for the second well is expressed by two coordinates, x_j and y_j. Aside from these two areas, four further, insulated fixed well positions are considered in this case, which are labeled N1, N2, W5*, and W7* (Fig. 5).

The second "*fixed and moving well*" case (MW_{big}) is intended to explore the wider surroundings of the current extraction system for recommendable well placement locations (installation of one additional well: $J = 1$). The range of its pumping rate, Q_j^{new}, is limited to 5% and 110% of the mean pumping rate (per well) of the reference case (55.3 m^3/h, Eq. (3)). The boundaries of the well placement area coincide with the area of interest (Figs. 3 and 5), and are expressed in Eqs. (4) and (5) by $x_{j,low}$ (west), $x_{j,up}$ (east) $y_{j,low}$ (south), and $y_{j,up}$ (north).

The drawdown constraints at nodes 'a–x' (Fig. 5) are expressed as multiplicative penalty P (Eq. (1)):

$$P = 10^{10\ k-\max_{z}(\Delta v_z)} \qquad (6)$$

The value of factor P is 1 when the candidate well layout yields a water table surface that complies with all predefined targets expressed as maximum values of water table level. If a well layout does not comply with all constraints (indexed by z), the k-highest violation $10\ k-\max_{z}(\Delta v_z)$ is selected and set as exponent in P (Eq. (6)). This exponential formulation provides a severe penalization, which comes into force already at small deviations from the desired levels (see Bayer and Finkel, 2004).

In the reference scenario, compliance with drawdown targets at all 24 constraint nodes is required ($k = 1$, i.e., $P = 10^{10\max_{z}(\Delta v_z)}$). In two further scenarios, the calculation of P was slightly modified to allow for violation of one (i.e., $k = 2$) or two (i.e., $k = 3$) constraints, respectively. This means that the maximal (and second maximal) constraint violations are simply ignored for calculating P. Since the nodes where these violations occur are case-specific, they cannot be specified in advance and their identification rather represents an output of the optimization procedure. This way, the modification of P enables the detection of the most relevant drawdown constraints for the optimized well layout and, what is more, the computation of the relative benefit from relaxing the drawdown objectives at such nodes.

To minimize the case-specific objective functions, numerous solvers are available. The purpose of this study was to concentrate on one robust optimization algorithm, which can efficiently tackle both fixed and moving well problems. Due to the experience from theoretical studies (e.g., Bayer and Finkel, 2007), a heuristic optimization algorithm from the family of evolution strategies, which represents one of the main branches of evolutionary algorithms, is used. Evolutionary algorithms are direct, probabilistic search and optimization algorithms. The aim of evolutionary algorithms is to use a natural phenomenon such as birth or death, variation and selection, in an iterative, respectively, generational loop (Beyer and Schwefel, 2002). Evolution strategies are particularly suitable for search problems in which global minimization or maximization of a complex non-linear objective function is required. During the optimization procedure, iterative search steps are taken by stochastic variation, so-called mutation, of a recombination of points (i.e., here well layouts) examined so far. In detail, the best μ (parents) out of a number of λ (i.e., the population size) new search points are selected in a generational manner to continue (survival of the fittest). A main strength of evolution strategies is their capacity to self-adapt. This means that the optimization not only takes place on decision variables, but also on strategy parameters, which determine the mutation distribution. The latter defines the degree of mutation and is updated each new generation (Bäck, 1996; Beyer and Schwefel, 2002).

Here, the CMA-ES algorithm ("evolution strategy with covariance matrix adaptation") is used. It is a modern variant of evolu-

Table 1
Settings for CMA-ES application for "fixed well" (FW), and the "fixed and moving well" cases MW_{small} and MW_{big}.

Case		No. of fixed wells	No. of moving wells	No. of decision parameters	λ (population size)	μ (offspring)	Iterations per optimization run
Fixed wells	FW	13	0	13	11	5	4000
Fixed and moving wells (small)	MW_{small}	17	2	22	13	6	8000
Fixed and moving wells (big)	MW_{big}	13	1	16	12	6	5000

tion strategies, which is gaining interest due to its promising search capabilities, both locally and globally (Hansen and Ostermeier, 2001; Hansen et al., 2003; Kern et al., 2004). According to Hansen and Ostermeier (2001), a population size of ca. $\lambda = 4 + 3\ln(N)$ and a number of parents of $\mu = \lambda/2$ is recommendable. It is also considered ideal for similar well placement problems (Bayer and Finkel, 2004, 2007). This means that λ and μ should be oriented at the number of decision variables, that is the problem dimension, *N*, of a particular problem. The well-case-specific settings for this study are listed in Table 1. For the further CMA-ES strategy parameters that control the search mechanism, default values as recommended by Hansen et al. (2003) were chosen to guarantee a robust application.

Fig. 7 summarizes the overall simulation–optimization concept. After selecting one of the three cases and defining decision space and constraints, the CMA-ES is initialized. This means that optimization algorithm specific strategy parameters are set and then the optimization procedure is started. During one optimization run, the CMA-ES iteratively tests candidate solutions (well layouts) which are assessed by running the groundwater model. With each iteration, a set of λ well layouts representing the actual generation is evaluated, ranked, and then the new information of the μ best is used to suggest the next generation. In this way, the solver tries to find an "intelligent" way through the decision space to converge to the global optimum. Only a small fraction of all possible well combinations are tested, and so the computational burden is held low. However, such an approach has only limited reliability in detecting the optimum after a predefined number of iterations, as only part of the decision space is investigated. Therefore, it is recommended that the optimization procedure is restarted several times, preferably with different starting search points, to increase the probability of finding the optimum. Here, for each scenario that is optimized, five different, randomly initialized optimization runs were conducted.

Although evolutionary algorithms are robust solvers that are applicable to a broad range of different problems, their performance may vary significantly. Of special importance is the problem-specific convergence time, i.e., the number of iterations required to converge to the (expected) optimum. For combined simulation–optimization applications, the use of time-consuming models is commonly prohibitive for detailed analysis of the characteristics of the respective objective function, its variability, non-linearity and (non-) convexity (i.e., the fitness landscape). If possible, test runs can help to appropriately tune the optimization algorithm and get a first insight into its performance. For the well layout problem examined in this study, a number of test runs aided in configuring the settings optimization procedure. In particular, an apposite number of maximum objective function evaluations (i.e., iterations) per optimization run were determined, which is chosen as termination criterion to cease the CMA-ES. As listed in Table 1, each optimization run involves 4000 (FW), 5000 (MW_{big}), and 8000 (MW_{small}) iterations, reflecting the different dimensionality of each case. These values are set substantially higher than the expected required number in order to capture possible optimization runs with late convergence. These rather conservative settings are viable due to the low run time of the groundwater model, which is only a few seconds.

Results

The well layout is first optimized for the fixed well case, FW. This case represents the same 13 wells as for the reference case, i.e., those wells that are currently in operation. All constraint nodes, 'a'–'x', are considered in order to examine whether the existing system can be improved by merely modifying the well-specific extraction rates, while fulfilling the same design criteria as given for the reference case. After five optimization runs, the best well layout found requires a total extraction rate $Q_{tot,FW} = 509.9\ m^3/h$, which means savings of 6.8% compared with the reference case (Table 2). As depicted by the bar graph in

Table 2
Total pumping rates (m^3/h) of reference case, and the optimized well layouts for "fixed well" (FW), and the "fixed and moving well" cases MW_{small} and MW_{big}.

Case	No. of neglected constraint nodes		
	0	1	2
Ref. case	543.3		
FW	509.9	497.7	442.9
MW_{small}	499.0	487.2	437.2
MW_{big}	495.6	404.2	400.1

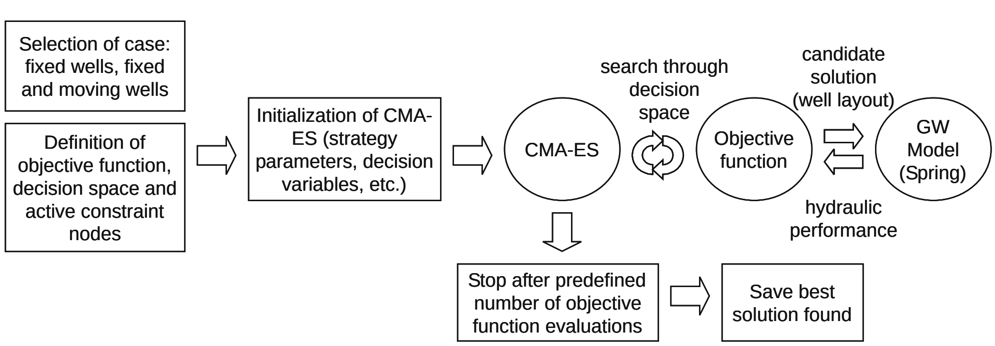

Figure 7. Flow chart illustrating the procedural elements of combined simulation–optimization framework using evolution strategies (CMA-ES).

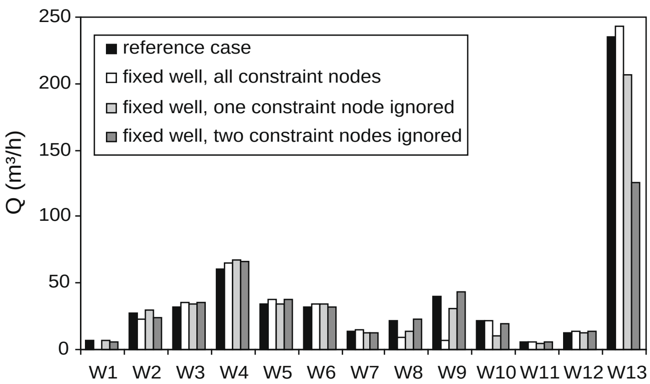

Figure 8. Pumping rates of wells W1–13 for the reference case and the optimized variants of the fixed well case.

Fig. 8, space to lower the pumping rates of W8–9 in the northern center of the area of interest is particularly evident. Simultaneously, the rates of the well gallery W3–6, of W7, and of the horizontal well W13, are slightly increased (Fig. 5). For some wells, the pumping rate reaches a maximum of 110% of the rate given for the reference case. Here, hitting the boundary of the decision space indicates that further potential savings may be utilizable by technically increasing the well capacity.

As an illustration of the CMA-ES performance, the five convergence curves of the optimization runs are shown in Fig. 9. The algorithm already converges within the first 1000 iterations close to the best solution found, which is expected to be close to the global optimum as it is reproduced by the different optimization runs. This fast convergence demonstrates an excellent CMA-ES performance, and reflects the benefit of appropriately defined ranges for the decision variables, that is, the acceptable pumping rate ranges, which are set to those of the reference case. The improvement of the system's pumping rate distribution shows the suitability of the algorithmic optimization procedure for further adjustment of even those systems that were soundly configured before.

As mentioned above, we also analyzed the role of the optimization constraints as given in terms of drawdown targets. Of special interest to the Walsum site is the potential of relaxing the given drawdown design criteria. One way to assess this potential could

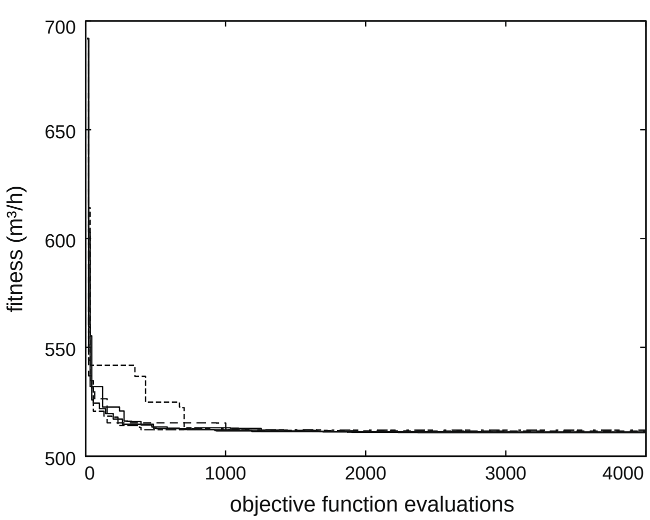

Figure 9. Fitness convergence curves for multiple CMA-ES runs for optimization of fixed well (FW) scenario.

be to simply increase the groundwater table limits at all nodes by a defined relative or absolute value, and then to optimize the system again. Alternatively, acceptance of violating one or more constraints can be accounted for in the formulation of the penalty, P (Eq. (6)), as was described above. This means that the objective is now to optimize the well layout while groundwater table levels may be above the desired limits at a specified number of locations. Since this relaxation is explicitly expressed by the formulation and calculation of the penalty in the objective function, the optimization algorithm automatically identifies the constraint node that should be ignored.

Fig. 8 reveals changes in the individual well-specific pumping rates, if the well layouts are optimized while one or two drawdown constraint nodes are ignored. Neglecting one node yields an extraction system with $Q_{tot,FW-1} = 497.7\ m^3/h$, which is only a slight improvement compared to the optimized pumping rate $Q_{tot,FW} = 509.9\ m^3/h$ complying with all drawdown constraints. In contrast, the total pumping rate can be significantly reduced by neglecting one more constraint node. In this case, the required total pumping rate drops to $Q_{tot,FW-2} = 442.9\ m^3/h$, which is only 82% of the rate calculated for the reference case. The improvements for both new solutions are mainly achieved by decreasing the pumping rate of W13, that is, the horizontal well which represents the most productive well of all. Its pumping rate is nearly halved, whereas the rates of the other wells do not substantially change. Accordingly, the nodes where the water table is not sufficiently lowered are located in vicinity of W13.

If one constraint node is ignored, the groundwater table at node 'r', which has to be decreased by more than 2 m (compared to no pumping), is 0.09 m above the desired level. In case of disregarding two constraint nodes, in addition to node 'r', the node located closest to W13, node 'v', is identified as the second "binding" constraint. Reflecting the significant reduction of the pumping rate of W13, the water table levels at node 'v' and 'r' considerably exceed the given limits (about 40 cm at both locations). In reality this case is only possible by carrying out other suitable precautions to keep the basements of the buildings around W13 dry. Other nodes surrounding W13, such as at nodes 'u', 'w', and 'x', are apparently less restrictive than 'v' and 'r' and, hence, not violated (see Fig. 5).

The next step to further optimize the current system was to consider the addition of a given number of further wells ($J = 6$) at predefined placement locations (MW_{small}). The new wells are named after the closest existing wells (e.g., W1*, W5*, W12*) or, if located in distant areas, this is stressed by "N" (wells N1, N2). The benefit of additional wells, however, is limited (Fig. 10). The required total extraction rate could be reduced to $Q_{tot,MWsmall} = 499\ m^3/h$, which means further savings of only 2% of $Q_{tot,ref}$ compared to the fixed well case. This is achieved by lowering the pumping rates at wells W1–11, except W5. The latter is located in the northern center together with W4 and adjacent new well W5*, which represent the most active wells here. Obviously it is desirable to locally concentrate the highest pumping rates instead of the linearly distributed original configuration. The constraints imposed at the northwestern area ('a'–'e') are now fulfilled by employing a new well, N1. This well is positioned at constraint node 'e' and extracts at a comparatively low rate (15 m^3/h). Another new well with substantial extraction rate, N2, is suggested in the south. Apparently the well assists in achieving the drawdown at the constraint nodes 'h'–'p' and compensating the decreased extraction rate of the horizontal well (Fig. 5). The other potential new wells such as W1* along the existing well gallery W1 to W6, W7* near W7, and W9* around W8 and W9, are not active, reflecting that the existing wells in these areas are already sufficient for achieving the given drawdown goals.

If one constraint node is ignored, pumping rate can be further reduced to $Q_{tot,MWsmall-1} = 487\ m^3/h$ (Table 2). This can mainly be

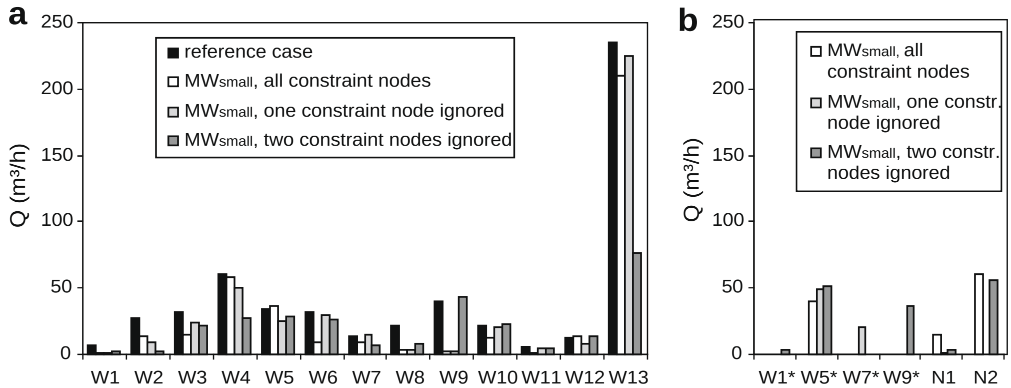

Figure 10. Pumping rates of wells W1–13 for the reference case and the optimized variants of the fixed and moving well case MW_{small}. New wells for MW_{small} are depicted in the right diagram.

attributed to utilizing W7* and neglecting N1 and N2 compared with the result for considering all drawdown limits. Again, similar to the FW case, the groundwater table is insufficiently lowered at node 'r'. For the optimized solution, the water table lies 20 cm above the given drawdown target. For the scenario of two constraint nodes being ignored, node 'v' is selected as second strongest constraint. The respective optimized well layout stresses well W5*, as is also observed for more restrictive scenarios MW_{small} and $MW_{small-1}$ (Fig. 10). Interestingly, W9* is now activated and also the adjacent wells W9–11 come more into force. Additionally, the southern well N2 now extracts at a rate $Q_{N2} > 50\ m^3/h$. This can be seen as balance to the mitigated regional effect of the horizontal well W13. The extraction rate of the latter has been reduced to nearly 1/3 of that of the reference case at the expense of particularly high water levels at the proximate surrounding. At node 'r', the resulting water table is 37 cm above the given target, and, at node 'v', it is even exceeds it by 56 cm. However, again, this case is only realistic when realizing suitable precautions which keep the basements free of groundwater.

The highest freedom in positioning new wells is specified by the second "*fixed and moving well*" case MW_{big}, where one additional well can be selected within the area of interest without any further limitation with respect to the position. Although only one well is added to the existing configuration of the extraction wells, the optimized well layout requires the lowest total extraction rate of $Q_{MWbig} = 495.6\ m^3/h$, compared with the other cases (Table 2). Fig. 11 demonstrates that pumping rates of vertical wells show only little changes as compared to the reference case. Decreased rates at W2 and W9 are most noticeable, and can be attributed to the fact that no constraint nodes are located in their vicinity. Highest benefit is gained from lowering the extraction rate of the horizontal well, W13. In order to avoid an overly significant local increase of the water table in the eastern area around W13 as a result of the well's lowered extraction rate, the location of the new well W12* is very close to nodes 'r' and 'v', which had previously been detected as the crucial constraint.

If one or two drawdown targets are neglected, the new well moves about 20 m in north-east direction from W12* to new location W12′. In this scenario, W12′ extracts at maximal rate of 60.8 m^3/h, while the horizontal well is nearly shut down. Consequently, significantly higher water levels than originally sought would be established in the eastern area under this scenario. However, compared with other, earlier, cases, constraint node 'r' does not appear to be stringent here as the close new well ensures sufficient drawdown at this spot. Instead, the water table would rise 73 cm above the targeted level at node 'v'. If two nodes can be ignored, node 'u' is selected as second most stringent constraint. The target violation is relatively small and amounts to 3 cm while the violation at node 'v' increases to 77 cm. Comparison of Figs. 12 and 6 illustrates that the groundwater table increases regionally within the entire area of interest compared to the reference case. This means that, to the disadvantage of targets in 'u' and 'v', drawdown can be relaxed in most areas, and explains why the new well layout significantly improves the extraction system. The total pumping rates are $Q_{tot,MWbig-1} = 404.2\ m^3/h$ and $Q_{tot,MWbig-2} = 400.1\ m^3/h$, for disregarding one or two constraint nodes, respectively. These represent savings of about 26% of the total extraction rate as compared to the reference case.

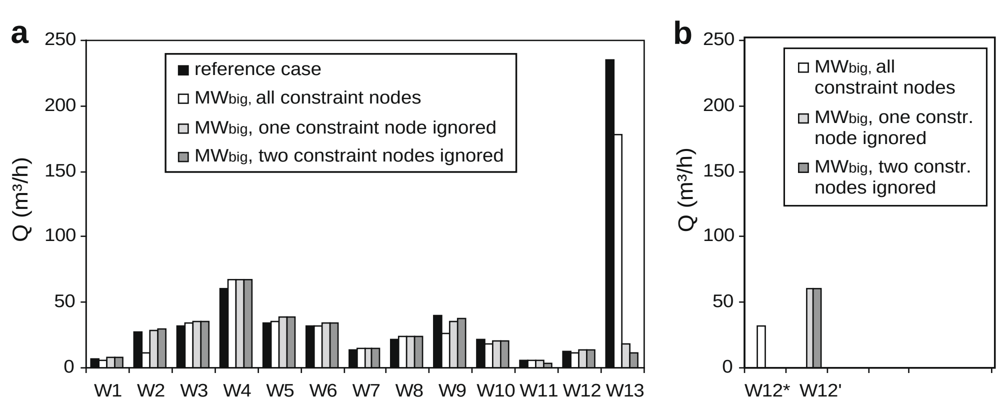

Figure 11. Pumping rates of wells W1–13 for the reference case and the optimized variants of the fixed and moving well case MW_{big}. New wells for MW_{big} are depicted in the right diagram.

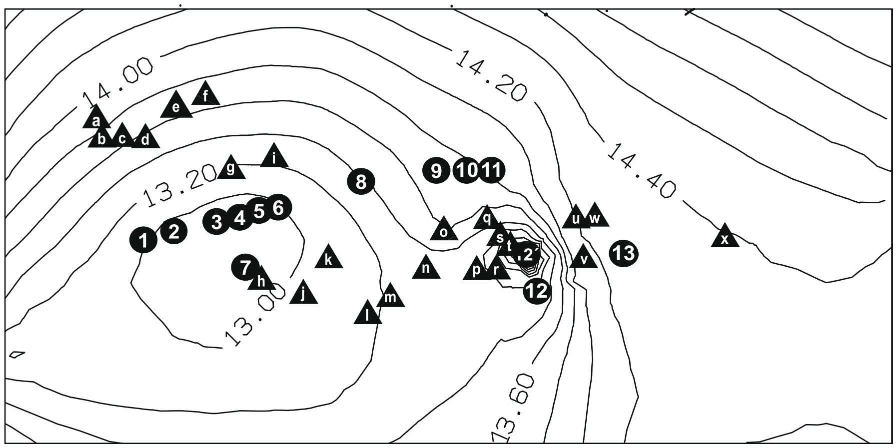

Figure 12. Head contours within "area of interest" for fixed and moving well case MW_{big}, when constraints 'u' and 'v' are ignored. The new well 'W12' is shown in addition to constraint positions (alphabetic, triangles) and well locations for the reference case (W1–12, circles), as depicted in Fig. 5.

Conclusions

In former underground mining areas, a common problem is subsidence of the ground and relative rise of the groundwater table. In populated areas, continuous pumping of groundwater is often the only solution to prevent damages to buildings and infrastructure. Due to the typically large size of the affected areas, immense technical, as well as economic, efforts are required for continuous regional drawdown of the groundwater table. At the site studied in this paper, Aldenrade-Walsum in the city of Duisburg, Germany, more than 4.45 million m^3 of water are discharged annually. Given the huge pumping rate, it is obvious that even slight improvements in the system layout may lead to significant economic benefits.

In this study, combined simulation–optimization has been applied to improve the extraction well layout currently installed in Aldenrade-Walsum. Different design criteria were considered for formulating purpose-built objective functions that are solved by evolution strategy. In fact, this study represents the first application of this type of optimization algorithm in the area of evolutionary algorithms on a real field site. The variant used, the evolution strategy with covariance matrix adaptation (CMA-ES), showed to be efficient in improving the pumping system. A particularly attractive feature is that no algorithm-specific testing was necessary before conducting the optimization. Evolution strategies are formulated as self-adaptive methods. They work reliably with default settings of the algorithm-specific strategy parameters that control the typical evolutionary operators such as mutation, recombination and selection.

Diverse design criteria for optimizing the well layout at Aldenrade-Walsum are defined, that is, acceptable groundwater table levels, well positions, and well numbers. Based on these, optimization scenarios are set up that yield a range of alternative well layouts. The latter are compared to the system in action, the reference case, by computing the relative differences in well-specific and total extraction rates. The configuration of the reference case has been adjusted and extended by experts over more than 30 years directed by the situation in this mining area.

It is demonstrated that the system in operation could be improved simply by optimally adjusting the individual pumping rates of the existing wells. A pumpage of more than 300,000 m^3 (6.8% of the total rate) can be saved annually without compromising any of the given design criteria. If the installation of additional wells is considered, the potential savings increase to nearly 9%. Two new well locations proved to be especially recommendable (W5* and N2, Fig. 5). Of course, before a new well is implemented in the field, the savings from reduced pumping rate has to be balanced with the additional costs for well installation. Interestingly, installation of well W5* has, meanwhile, also been considered in practice, independent of the results of this study. This further validates the aptness of the presented combined simulation–optimization procedure.

We also used combined simulation–optimization to investigate the potential of further improving the optimized solutions. In detail, we examined how optimal solutions do change if critical groundwater table drawdown targets are ignored. This was done automatically by making use of different penalty functions which allow the violation of one or two drawdown constraints during the optimization. Note that the location of these critical constraints is not predetermined but is automatically identified during the optimization. Such an approach can be compared to common chance-constraint formulations, but is not conventional and has not yet been utilized to examine the improvement potential of groundwater abstraction systems. Insight into the sensitive features of a system can be as important as the configuration of the optimized system itself. Therefore the findings of this study establish a reliable basis to guide future modifications of the system in action.

Acknowledgements

This work was supported by a research grant from the German Research Foundation (Deutsche Forschungsgemeinschaft), Contract No. BA 2850/1-2, and by the GWAT-LCA project within the 7th framework program (Contract No. PIEF-GA-2008-220620). Two reviewers helped to improve the presentation. The diligent assistance of Claudius M. Bürger, Anna Bentz, and Margaret Hass in preparing the manuscript is gratefully acknowledged.

References

Bäck, T., 1996. Evolutionary Algorithms in Theory and Practice: Evolution Strategies, Evolutionary Programming, Genetic Algorithms. Oxford University Press, New York. 314p.

Baumgart, H.C., Sperling, F., Stemplewski, J., 2003. River basin management, described for the example of the Emschergenossenschaft. Water Sci. Technol. 47 (7–8), 141–147.

Bayer, P., Bürger, C.M., Finkel, M., 2008. Computationally efficient stochastic optimization using multiple realizations. Adv. Water Resour. 31 (2), 399–417. doi:10.1016/j.advwatres.2007.09.004.

Bayer, P., Finkel, M., 2007. Optimization of concentration control by evolution strategies: formulation, application, and assessment of remedial solutions. Water Resour. Res. 43, W02410. doi:10.1029/2005WR004753.

Bayer, P., Finkel, M., 2004. Evolutionary algorithms for the optimization of advective control of contaminated aquifer zones. Water Resour. Res. 40. doi:10:1029/2003WR002675.

Bürger, C.M., Bayer, P., Finkel, M., 2007. Algorithmic funnel-and-gate system design optimization. Water Resour. Res. 43, W08426. doi:10.1029/2006WR005058, 2007.

Beyer, H.-G., Schwefel, H.-P., 2002. Evolution strategies – a comprehensive introduction. Nat. Comput. 1, 3–52.

Carbognin, L., Teatini, P., Tosi, L., 2004. Eustacy and land subsidence in the Venice Lagoon at the beginning of the new millennium. J. Marine Syst. 51 (1–4), 345–353.

Chu, H.J., Hsiao, C.T., Chang, L.C., 2005. Optimal remediation design in groundwater systems by intelligent techniques. Lect. Notes Artif. Int. 3682, 628–634.

DMT, 2005. Bericht zum Pumpversuch im Bereich der Pumpanlage Du-Aldenrade. Deutsche Montan Technologie GmbH, Essen, 34 S.

DSK, 2002. Bergwerk Walsum Erläuterungsbericht und allgemein verständlich Zusammenfassung zum UVP-pflichtigen Rahmenbetriebsplan für den untertägigen Abbau vom 01.01.2002 bis 31.12.2019, (retrieved 2.10.06). <http://www.bergschaden-kohlebergbau.de/ruhr/RBPWALS.rtf>.

Emschergenossenschaft, 2004. Antrag gemäß §§ 2, 3 und 7 WHG zur Entnahmeerhöhung von Grundwasser zur Sicherstellung der Flurabstände im Bereich der Pumpanlage Du-Aldenrade der Stadt Duisburg. Emschergenossenschaft, 2004 (not published).

Freeze, R.A., Gorelick, S.M., 1999. Convergence of stochastic optimization and decision analysis in the engineering design of aquifer remediation. Ground Water 37 (6), 934–954.

Guan, J.B., Aral, M.M., 1999. Optimal remediation with well locations and pumping rates selected as continuous decision variables. J. Hydrol. 221, 20–42.

Hansen, N., Ostermeier, A., 2001. Completely derandomized self-adaptation in evolution strategies. Evol. Comput. 9 (2), 159–195.

Hansen, N., Müller, S.D., Koumoutsakos, P., 2003. Reducing the time complexity of the derandomized evolution strategy with covariance matrix adaptation (CMA-ES). Evol. Comput. 11 (1), 1–18.

Katsifarakis, K.L., Petala, Z., 2006. Combining genetic algorithms and boundary elements to optimize coastal aquifers' management. J. Hydrol. 327 (1–2), 200–207.

Kern, S., Müller, S.D., Hansen, N., Büche, D., Ocenasek, J., Koumoutsakos, P., 2004. Learning probability distributions in continuous evolutionary algorithms – a comparative review. Nat. Comput. 3 (1), 77–112.

Mantoglou, A., Kourakos, G., 2007. Optimal groundwater remediation under uncertainty using multi-objective optimization. Water Resour. Manag. doi:10.1007/s11269-006-9109-0.

Marino, G.G., Abdel-Maksoud, M.G., 2006. Protection measures against mine subsidence taken at a building site. J. Mater. Civ. Eng. 18, 152–160.

Morton, R.A., 2003. An overview of coastal land loss: with emphasis on the Southeastern United States. US Geological Survey open-file report 03–337, 29 pp.

Park, C.H., Aral, M.M., 2004. Multi-objective optimization of pumping rates and well placement in coastal aquifers. J. Hydrol. 290 (1–2), 80–99.

Papadopoulou, M.P., Pinder, G.F., Karatzas, G.P., 2007. Flexible time-varying optimization methodology for the solution of groundwater management problems. Eur. J. Oper. Res. 180 (2), 770–785.

Phien-wej, N., Giao, P.H., Nutalaya, P., 2006. Land subsidence in Bangkok. Thailand Eng. Geol. 82 (4), 187–201.

Roosmann, R., Gorczyk, J., Mauersberger, F., Nickel, S., Busch, W., 2003. Modeling spatiotemporal objects and processes as a basis for monitoring the environmental influences caused by deep hard coal mining. In: Troch, I., Breitenegger, F. (Eds.), Proceedings 4th MATHMOD Vienna, February 2003. ARGESIM-Verlag, Wien, pp. 598–608 (ARGESIM-Report 24; vol. 1, S. 95 und vol. 2 (CD)).

SPRING, 2004. User Manual, Version 3.10. delta-h Ingenieurgesellschaft, Bochum.

Zheng, C., Wang, P.P., 2002. A field demonstration of the simulation–optimization approach for remediation system design. Ground Water 40 (3), 258–265.